Biochimica et Biophysica Acta 1787 (2009) 1170–1178

Contents lists available at ScienceDirect

Biochimica et Biophysica Acta

journal homepage: www.elsevier.com/locate/bbabio

Spectral characteristic of fluorescence induction in a model cyanobacterium, *Synechococcus* sp. (PCC 7942) ☆

Radek Kaňa [a,b,*], Ondřej Prášil [a,b], Ondřej Komárek [a,b,e], George C. Papageorgiou [c], Govindjee [d]

[a] *Laboratory of Photosynthesis, Institute of Microbiology, Academy of Sciences Czech Republic, Třeboň, Czech Republic*
[b] *Institute of Physical Biology and Faculty of Biology, University of South Bohemia in České Budějovice, Czech Republic*
[c] *National Center for Scientific Research Demokritos, Institute of Biology, 153 10 Athens, Greece*
[d] *Department of Plant Biology, Department of Biochemistry and Center of Biophysics and Computational Biology, University of Illinois at Urbana-Champaign, 265 Morrill Hall, 505 South Goodwin Avenue, Urbana, IL 61801-3707, USA*
[e] *Institute of System Biology and Ecology, Academy of Sciences Czech Republic, Nové Hrady 136, 37 333, Czech Republic*

ARTICLE INFO

Article history:
Received 5 December 2008
Received in revised form 24 March 2009
Accepted 15 April 2009
Available online 3 May 2009

Keywords:
Fluorescence induction
Cyanobacterium
PCC 7942
Phycobilisome
State transition

ABSTRACT

We present here three-dimensional time-wavelength-intensity displays of changes in variable fluorescence, during the O(JI)PSMT transient, observed in cyanobacterium at room temperature. We were able to measure contributions of individual chromophores to fluorescence spectra at various times of fluorescence induction (FI). The method was applied to a freshwater cyanobacterium, *Synechococcus* sp. (PCC 7942). Analysis of our experimental results provides the following new conclusions: (i) the main chlorophyll (Chl) a emission band at ~685 nm that originates in Photosystem (PS) II exhibits typical fast (OPS) and slow (SMT) FI kinetics with both orange (622 nm) and blue (464 nm) excitation. (ii) Similar kinetics are exhibited for its far-red emission satellite band centered at ~745 nm, where the PS II contribution predominates. (iii) A significant OPS-SMT-type kinetics of C-phycocyanin emission at ~650 nm are observed with the blue light excitation, but not with orange light excitation where the signal rose only slightly to a maximum. The induction of F650 was not caused by an admixture of the F685 fluorescence and thus our data show light-inducible and dark-reversible changes of phycobilin fluorescence *in vivo*. We discuss possible interpretations of this new observation.

© 2009 Elsevier B.V. All rights reserved.

1. Introduction

A dilute solution of chlorophyll (Chl) a emits fluorescence, the intensity of which is constant with time of illumination. In contrast, the intensity of the Chl a fluorescence which photosynthetic cells emit changes with time, tracing characteristic and reproducible kinetic patterns throughout illumination intervals that extend from sub-picosecond (ps) to tens of minutes, and even longer (reviewed by Papageorgiou et al. [1]). Chl a fluorescence is affected by physico-chemical and physiological processes that occur within and across the thylakoid membranes and relate to photosynthesis; in addition, syntheses and the degradations of holochromic proteins affect the stoichiometry of photosystems and the sizes of their antennae [2].

The ps-to-min time course of Chl a fluorescence is rich in information on several disparate photosynthesis-related levels that include: ultrafast intermolecular exciton transfer, exciton trapping and charge stabilization (~sub-ps to ns; reviewed by Tyystjärvi and Vass [3]); ground state electron and proton transport processes (~μs to s; reviewed by Bruce and Vasil'ev [4], Kramer et al. [5]); and intersystem holochrome movements (~s to min; in the so-called state transitions, reviewed by Mullineaux and Emlyn-Jones [6]). In particular, the μs to min segment of this Chl a fluorescence time course, commonly referred to as fluorescence induction (FI), has been extensively investigated and exploited (see reviews by Papageorgiou et al. [1], Mullineaux and Emlyn-Jones [6], Govindjee [7], Lazár [8], and Strasser et al. [9]).

We studied the FI properties of the freshwater cyanobacterium *Synechococcus* sp. PCC 7942 (formerly *Anacystis nidulans* R2), a model organism in photosynthesis research. The thylakoid membranes of this prokaryote contain the core antenna Chl *a*-protein complexes of Photosystem (PS) I and PS II, which are common in all oxyphototrophs, but lack the peripheral trans-membrane light-harvesting Chl a, b complexes (LHC) of the eukaryotic cells. Instead, they use for light harvesting the phycobiliproteins, C-phycocyanin (CPC) and allophycocyanin (APC), assembled into externally-attached organelles, the phycobilisomes, PBS (reviewed by MacColl [10] and Adir [11]).

Electronic excitation that is generated in the light-harvesting system of *Synechococcus* (in the extrinsic phycobiliproteins or in the intrinsic PS I and PS II Chl a holochromes) is transferred to the reaction center of PS I or PS II (PS I RC, PS II RC) that initiates photosynthetic electron transport [12]. Electronic excitation is also dissipated as heat and as fluorescence emission that can be used effectively to monitor

☆ Dedicated to Prof. Dr. Achim Trebst at his 80th birthday on June 9, 2009.

* Corresponding author. Tel.: +420 384340436; fax: +420 384340415.
E-mail address: kana@alga.cz (R. Kaňa).

0005-2728/$ – see front matter © 2009 Elsevier B.V. All rights reserved.
doi:10.1016/j.bbabio.2009.04.013

various photosynthetic processes. Selective excitation of Chl a by blue light generates fluorescence from the Chl a molecules of both PS II and PS I, while selective excitation of CPC (by orange light) generates broadband fluorescence from the CPC and APC proteins of the extrinsic PBS as well as from the intrinsic Chl a holochromes of PS II and PS I.

The regulation of electronic excitation and its distribution are reflected in FI pattern usually measured in the 690–700 nm spectral range that relates to changes in PS II photochemistry. The fast part of FI curve in cyanobacteria (first second of actinic irradiance) is rather shallow in comparison to the well-structured and dynamic OJIP kinetics in higher plant leaves [1]. The fast OJIPS transient is followed by a much slower fluorescence increase from the S-plateau to the M peak appearing tens of seconds after the onset of light. The SM rise of FI is dominant in cyanobacteria in contrast to the higher plants and green algae [1] and has been assigned mostly to an increased PBS → PS II excitation transfer for the following reasons: (i) it has been observed only in PBS-sensitized Chl a fluorescence [1]; (ii) it is usually much lower or is absent in higher plants, green algae and non-PBS-containing cyanobacteria [1] (iii) hyper-osmotic conditions block the SM rise in PBS-containing cyanobacteria reversibly, without blocking the OJIPS phase [13]; (iii) the SM rise can be observed also in the presence of DCMU (diuron, that blocks electron transfer from PS II to PS I), and this rules out the involvement of Q_B and the PQ-pool in it [14]. Blocking of the PBS → PS I excitation transfer enhances the SM rise (maximal PBS excitation ends up in PS II) and on the other hand stimulation of this transfer can fully abolish the SM rise as much less PBS excitation ends up in PS II [1,13]. This phenomenology suggests that the SM rise reflects the regulatory distribution of PBS excitation, which is known as state 2-to-state 1 transition (see e.g. [6] for review) since cyanobacteria tend to stay in the low fluorescence state 2 during dark and are transformed into the highly fluorescent state 1 during irradiation [13].

This FI measured at narrow spectral range results in two-dimensional displays of the momentary value of fluorescence intensity as a function of illumination time ($F_t = f(t)$) that reflects mostly photochemical events in PS II. However, modern diode-array equipment allows us to measure the entire emission spectrum within approx. 1 s that enables us to measure families of fluorescence spectra at various times of actinic light illumination together with fluorescence induction (FI) curves at various wavelengths. This can be then presented as three-dimensional diagrams in which the fluorescence intensity (F) is plotted against two independent variables, wavelength (λ) and time (t), namely displays of the function $F_t = \Phi(\lambda,t)$. The information content of the three-dimensional FI diagrams is richer than that of the two-dimensional $F_t = f(t)$ ones, thus this analysis provides us a clearer insight into the physicochemical and molecular events that lie behind the phenomenology of FI. To achieve this, we have spectrally resolved the characteristic SMT transient in cyanobacterium *Synechococcus* sp. PCC 7942 at characteristic wavelengths of emission of various chromophores (i.e. PS II, PS I, PBS). The 3-dimensional spectral characteristics of fluorescence induction ($F_t = \Phi(\lambda,t)$) were detected, for the first time, during the O(JI)PSMT transient, with selective excitation either of Chl *a* or of CPC. We discuss these results in the context of our present understanding of the regulation in excitation energy distribution in the pigment systems of cyanobacteria during photosynthetic induction.

2. Materials and methods

2.1. Photosynthetic organism

The freshwater cyanobacterium *Synechococcus* sp. PCC 7942 was cultivated in the batch mode in standard BG 11 medium under constant white light irradiance of 50 μmol photons m^{-2} s^{-1} of PAR (Photosynthetically Active Radiation) [15]. The cultures were periodically diluted with fresh medium.

2.2. Steady-state absorption and fluorescence spectra

Absorption spectra were recorded with a Unicam UV 550 (Thermospectronic, UK) spectrophotometer that was equipped with an integrating sphere. Cells were infiltrated on nitrocellulose membrane filters (pore diameter 0.6 μm; Pragochema, Czech Republic), and these filters were positioned in the integrating sphere. Absorbance was measured with a 4 nm detection bandwidth step in the 390 nm to 750 nm range.

Fluorescence emission spectra at 77 K were measured using an Aminco-Bowman Series 2 spectrofluorometer, in a standard instrument geometry. Dilute suspensions (in order to avoid fluorescence reabsorption) were first dark adapted at room temperature for ~15 min and then infiltrated on nitrocellulose membrane filters which were fitted in a sample holder and immersed in an optical Dewar flask filled with liquid nitrogen. Excitation was provided at two spectral bands, 438 nm and 580 nm, each with a 4 nm bandwidth. Fluorescence emission was scanned with a 4 nm bandwidth.

2.3. Fluorescence kinetics

Fluorescence induction measurements were performed with a Double-Modulation Fluorometer FL-100 (Photon Systems Instruments, Czech Republic); for details, see Trtílek et al. [16]. Actinic irradiance was provided by a set of photodiodes either at 464 nm (~200 μmol (photons) m^{-2} s^{-1}), or at 622 nm (~33 μmol (photons) m^{-2} s^{-1}) and fluorescence was detected in the 690–710 nm spectral range. Fluorescence was sampled continuously with logarithmically increasing intervals between measured points (55 points per every decade with a first point at 46 μs after the onset of exciting light). Before each measurement, *Synechococcus* cells were dark adapted for ≥15 min.

Simultaneous recordings of fluorescence spectra were performed with Spectrometer SM-9000 (Photon Systems Instruments, Czech Republic) that has a constant instrument response for all the used wavelengths. A light guide of the spectrometer was fitted to the cuvette of the FL-100 fluorometer in a geometry that allowed simultaneous detection of signal from FL-100 Fluorometer and SM-9000 Spectrometer. The dark current of the instrument was automatically subtracted before measurements. The F_o level spectra were collected for approximately 10 s at the low measuring light that the FL-100 Fluorometer provided (light intensity, <0.5 μmol (photons) m^{-2} s^{-1} of blue (464 nm) or of orange (622 nm) light). We note that the F_o level is the minimum fluorescence of the system, when the primary quinone acceptor, Q_A, of PS II is fully oxidized [1,7,9]. The spectral characteristics of the fluorescence emitted during the induction were detected at the actinic light provided by FL-100 Fluorometer, i.e., ~200 μmol (photons) m^{-2} s^{-1} of blue light or at ~33 μmol (photons) m^{-2} s^{-1} of orange light. The spectrophotometer, used in this research, allowed us to scan the entire emission spectra every 1 s for a total of 300 s (at a spectral bandwidth of 2 nm) simultaneously with the measurements of modulated fluorescence (see above).

2.4. Data analysis

Raw data of fluorescence emission spectra, measured by SM-9000 Spectrometer during slow FI were imported into analytical software Origin (version 8.0, OriginLab Corp., USA). All data were normalized to the changes in the intensity of excitation light. The spectrum of the excitation light was subtracted from the raw data before processing and then the analytical tools of Origin were used to construct the three-dimensional FI plots and to deconvolute the fluorescence

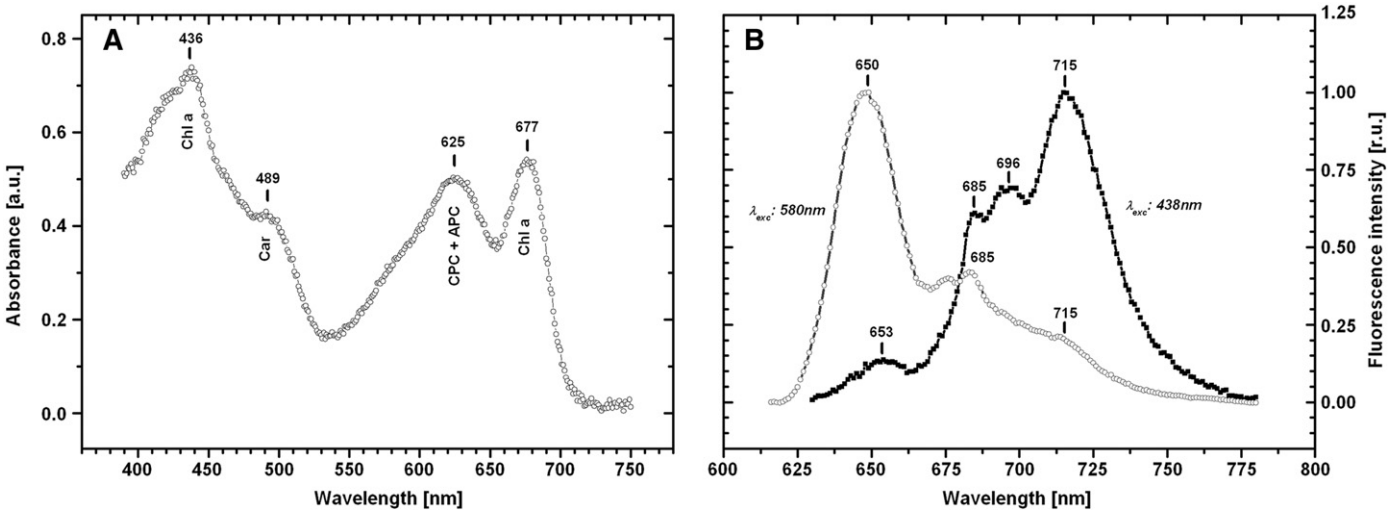

Fig. 1. Absorption (A) and fluorescence spectra (B) of *Synechococcus* sp. PCC 7942. Absorption of a cell suspension was recorded at room temperature; fluorescence of frozen cell suspension was measured at 77 K, following excitation either at 438 nm (closed circles) or at 580 nm (open circles). Displayed curves are average of three measurements. Cells were dark adapted for 15 min before each measurement.

emission spectra at particular times into their Gaussian components. In the latter process, band peaks and bandwidths were first taken as initial conditions for the fitting procedure but subsequently their particular values were adjusted using chi squared (χ^2) reduction. This approach allowed us to compare changes in the contribution of particular pigment–protein complexes during the course of FI.

3. Results

3.1. Absorption and emission spectra

Fig. 1A shows the room temperature absorption spectrum of a *Synechococcus* cell suspension and Fig. 1B fluorescence emission spectra of the same cell suspensions frozen at 77 K measured at 2 different wavelengths of excitation. The absorption band maxima and the main contributing chromophores are: 436 nm (mainly Chl a); 489 nm (mainly carotenoids); 625 nm (mainly CPC and APC); and 677 nm (mainly Chl a). Low temperature fluorescence was excited either at 438 nm where Chl a *in vivo* absorbs strongly [17,18] and CPC [19–21] plus APC [19,22] weakly, or at 580 nm where CPC [20,23] and APC [22,23] absorb strongly and Chl a less strongly [17,18]. These spectra are shown here in order to characterize the cyanobacterial cells we used in this research.

The two 77 K emission spectra are conspicuously different (Fig. 1B). Excitation at 438 nm generates two emission bands, F685 and F696, that originate from the Chls *a* of the CP43 and CP47 proteins of PS II [24], and one emission band, ~F715, that originates mostly from Chls a in PS I [25]. The smaller band at 653 nm is most likely directly excited CPC fluorescence. In contrast, the spectrum of the 580 nm excitation gives a prominent emission band, F650, that originates from CPC [19] and a smaller band around 675 nm that originates from APC-B [26] and the F685 emission band, which originates from Chls *a* of PS II, and contains also some APC emission, and finally a shoulder at 715 nm that can be assigned to Chls *a* of PS I [25]. The 696 nm Chl a emission band is not resolved under this excitation.

3.2. Fluorescence induction

Fig. 2 displays fluorescence induction (FI) curves recorded at room temperature with (15 min) dark pre-adapted *Synechococcus* cell suspensions. The cells were illuminated continuously either with the blue (464 nm), or with orange (622 nm) actinic light and fluorescence was detected in the spectral interval 690–710 nm ($F_{690-710}$). Since the blue excitation at 464 nm is not significantly absorbed by CPC [19–21] or by APC [22], only Chl a is excited directly by this blue excitation. The orange excitation at 622 nm is absorbed mainly by the phycobiliproteins that generates directly excited phycobiliprotein fluorescence and indirectly excited Chl a fluorescence due to excitation energy transfer from CPC → APC → Chl a [12].

The $F_{690-710}$ signal (presented in Fig. 2) contains mainly Chl *a* emission from PS II [cf. 24], with negligible amount of CPC [19,20] and APC emission [19,23]. There could be also Chl a emission from PS I [24]. According to e.g., Franck et al. ([27], experiments with leaves), the PS I fraction of the total Chl *a* fluorescence signal is maximal at F_o and minimal at F_m, suggesting that all, or most, of the variable Chl a fluorescence originates in PS II (see Itoh and Sugiura [28] for a review on PS I fluorescence). However, the constancy of the PS I fluorescence

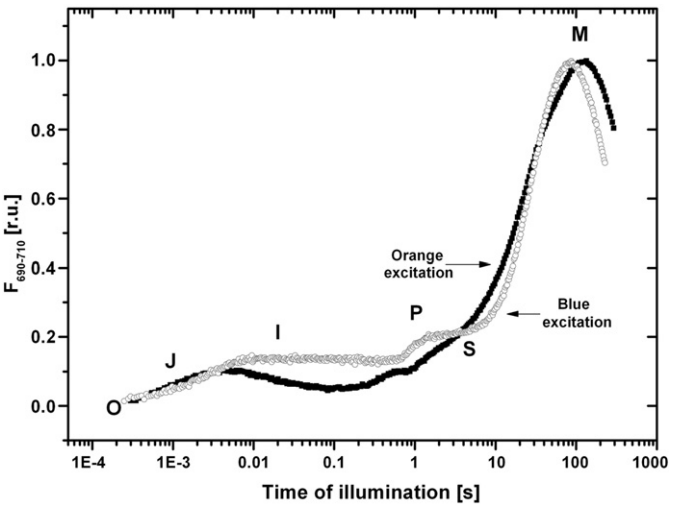

Fig. 2. Time course of chlorophyll *a* fluorescence (fluorescence induction, FI) from dark-pre-adapted *Synechococcus* sp. PCC 7942 suspension during continuous excitation at room temperature. Fluorescence was detected in the 690–710 nm range ($F_{690-710}$) with excitation either at 464 nm (200 μmol (photons) m^{-2} s^{-1}; blue actinic light) or at 622 nm (33 μmol (photons) m^{-2} s^{-1}; orange actinic light). The FI curves were normalized to equal M–O differences and the O level fluorescence was set to zero to allow us to compare blue light induced FI with FI after orange light excitation; r.u. on the ordinate stands for relative units; the nomenclature of time points (OJIPSM) follows that used earlier [1].

and the phycobilin fluorescence emissions in cyanobacteria, during FI (i.e., under continuous actinic illumination from μs to min), has not been proven rigorously.

The two curves shown in Fig. 2 were normalized (see the legend for details) to facilitate their comparison. In cyanobacteria, the 464 nm excitation is preferentially absorbed by PS I that contains more Chl *a* [29] than by PS II [30,31] and is stoichiometrically more abundant than PS II (PS I/PS II ≈ 2–5, according to Fujita et al. [31]). However, because PS I RC (P700) turns over faster than the PS II, it has lower fluorescence intensity than the PS II antenna. Therefore, Chl a fluorescence excited by blue actinic light at 464 nm is weaker in comparison to excitation by orange light at 622 nm (data not shown) as the orange light absorbed by CPC is primarily transferred to more fluorescent Chls *a* of PS II. This is indicated by a low temperature PS I emission band (F715) of dark adapted cells (Fig. 1B) where F715 (emission of PSI) is much weaker for 580 nm excitation than the PS II emission band (F685). The

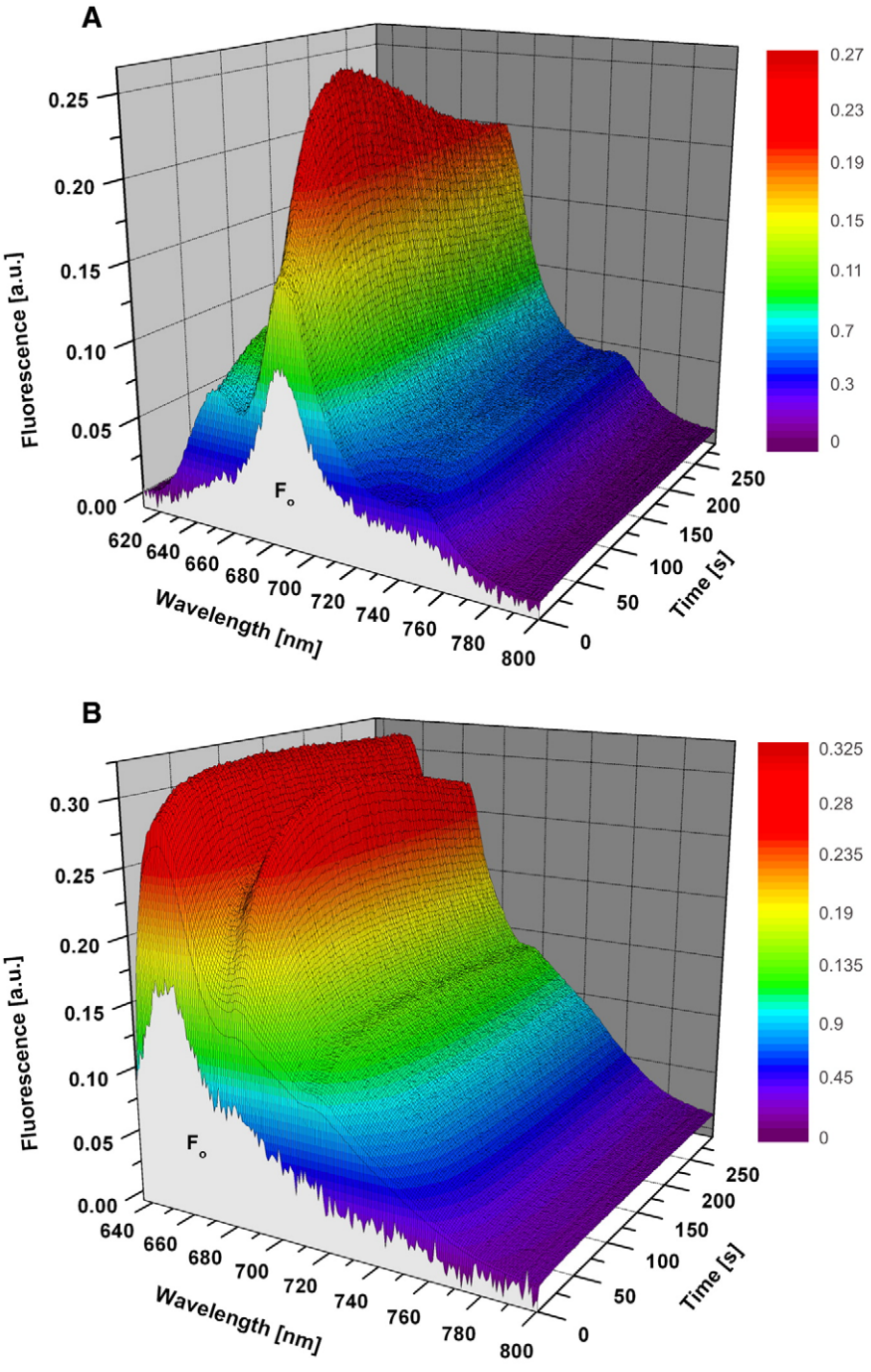

Fig. 3. Three-dimensional displays of fluorescence emitted by *Synechococcus* sp. PCC 7942 cells in suspension relative to the wavelength of fluorescence detection and the duration of actinic light illumination. At the beginning, F_o spectra of the dark adapted cells were recorded using weak measuring excitation (0.5 μmol(photons) m^{-2} s^{-1}) of blue (464 nm — panel A) or orange (622 nm — panel B) light. After the onset of actinic blue light (464 nm, ~200 μmol(photons) m^{-2} s^{-1}; panel A) or actinic orange illumination (622 nm, ~33 μmol (photons) m^{-2} s^{-1}; panel B), fluorescence spectra were recorded every second. Fluorescence intensity (*Z*-axis) is plotted against emission wavelength (*X*-axis) and illumination time (*Y*-axis). Artificial colors of the 3D plots represent the intensity of fluorescence at a particular time of fluorescence induction (see *Y*-axis) and at a particular wavelength (see *X*-axis). Slice parallel to the *XZ* plane is the room temperature fluorescence emission spectrum at a particular illumination time, while a slice parallel to the *YZ* plane can be interpreted as the time course of fluorescence at a particular wavelength. The data were obtained by spectrometer SM-9000 together with data presented in Fig. 2. a.u. on the *Z*-axis stands for arbitrary units.

F715 is the CPC-sensitized emission of PS I Chls *a* that represents the largest fraction of CPC excitation transferred to PS I. Therefore only a small fraction of the CPC excitation is transferred to the Chls *a* of PSI, and this fraction is largest in the dark adapted state of cyanobacteria (state 2) and smallest in the light-adapted state (state 1; see reviews in [1] and [18] and references cited therein).

Fluorescence kinetic patterns, such as those in Fig. 2 for excitation at 622 nm (orange), with a low-amplitude fast phase (OJIPS) and a dominant slow phase (SMT), are typical of PBS-containing cyanobacteria exposed to orange light. According to Fig. 2, a similar OJIPSMT fluorescence kinetic pattern [1] is also generated by exciting Chls *a* at 464 nm (blue). Despite their qualitative similarity, the two FI patterns are different both in the slow SMT phase and in the fast OJIPS phase. With excitation at 464 nm, the SM phase rises faster and M peak occurs ~30 s earlier than with excitation at 622 nm. We have also observed that the SM amplitude depends on the length of the dark pre-adaptation period; long dark pre-adaptation results in higher M peaks with blue light excitation but lower M peaks with orange light excitation (data not shown).

3.3. Spectral characteristic of fluorescence induction

The spectral characteristics of *in vivo* room temperature fluorescence induction for blue (464 nm) and for orange (622 nm) light excitation are shown in Fig. 3A and B, respectively. Fluorescence intensity is plotted in terms of color-coded contours. Slices parallel to the *XZ* plane represent fluorescence emission spectrum at a particular illumination time, while slices parallel to the *YZ* plane indicate the time course of fluorescence intensity at a particular wavelength (i.e., fluorescence induction). However, the three-dimensional figure masks some time-dependent changes. In order to overcome this, we have also reduced the three-dimensional representation to a two-dimensional one in which fluorescence intensity is depicted in terms of iso-emissive contour lines, and this is shown in Fig. 4A and B for blue excitation at 464 nm and orange excitation at 622 nm, respectively.

In Fig. 3A and B, the initial spectra (denoted as F_o) were recorded before the onset of actinic light using only low intensity excitation (below 0.5 μmol (photons) m^{-2} s^{-1}), which is too weak to initiate FI. The F_o spectrum with excitation at 464 nm (Fig. 3A) displays a dominant fluorescence band at ~682–686 nm (F685) contributed mostly by Chls *a* of PS II (plus a small contribution of APC-B), a lower band at ~650–655 nm (F650) contributed mostly by CPC and APC (plus a minor contribution by Chl *a*). There is also a broad Chl *a* fluorescence band in the ~710–780 region where we can discern two emission ranges: 710–720 nm (F710) contributed mostly by Chls *a* of PS I (and less by Chls *a* of PS II) and 730–750 nm (F745) that is a vibrational Chl *a* emission satellite contributed mostly by PS II and by PS I (see e.g. [25]). The choice of the use of 'F710' and 'F745' here and what follows is based on the deconvolution spectra, discussed later in the paper. The F_o spectrum, obtained after excitation at 622 nm (Fig. 3B), display is quite different than the one observed after 464 nm excitation: here, the F650 band (peak ~650–652 nm) is prominent and the F685 band (peak ~683 nm) is much weaker. There are also smaller far-red satellite bands of Chl *a* fluorescence emitted by PS I and PS II chlorophylls, F710 and F745, with the same origin as for the weak blue excitation at 464 nm (see above).

After recording the F_o spectra of the dark adapted cells (Fig. 3), the cells were subjected to continuous actinic illumination at 464 nm (200 μmol (photons) m^{-2} s^{-1}) or at 622 nm (33 μmol (photons) m^{-2} s^{-1}) and fluorescence spectra, spaced 1 s apart, were recorded. Strikingly differing spectral characteristics of fluorescence induction was the result. In the case of 464 nm exciting light (Figs. 3A and 4A), the F685 band rose clearly to a maximum in about 80–100 s and then declined according to the SMT pattern. Similarly, The F650 and F745 bands also rose after irradiation. Based on the raw experimental data, the F710 band seems to remain more or less unchanged. Similarly, in the case of the 622 nm exciting light (Figs. 3B and 4B), the rise and subsequent decline of F685 is also evident, together with an unexpected rise of the F650 band and its much slower subsequent decline compared to the F685 band. A possible kinetic behavior (i.e. FI) of the smaller F710 and F745 far-red bands could not be resolved from the raw datasets for both excitations because the more intense F650 and F685 bands mask the kinetics. Therefore, to further the spectral analysis of the FI kinetics we deconvoluted the recorded spectra into Gaussian sub-bands.

3.4. Emission spectra at fixed times of actinic illumination and their deconvolution

Fig. 5 displays fluorescence spectra at characteristic phases of FI time courses that were recorded with blue (464 nm, panel A) and with orange (622 nm, panel B) actinic lights. The most evident changes occur mainly, as expected, in the Chl a emission band of PS II (F685) but there are also visible variations in the long wavelength

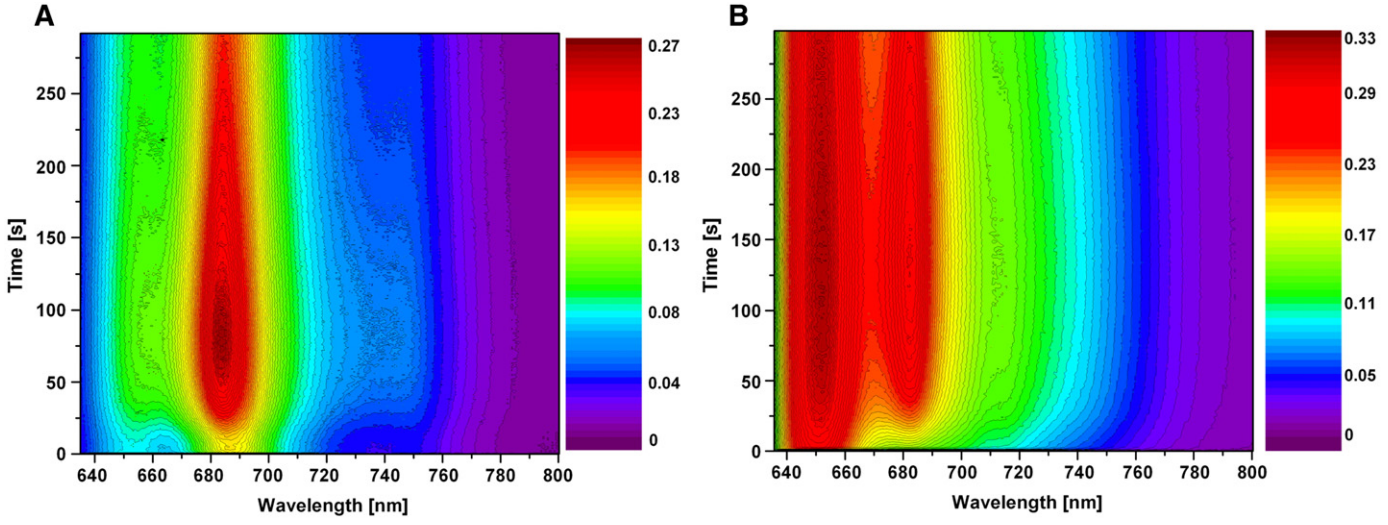

Fig. 4. Two-dimensional spectral characteristic of fluorescence induction (FI) obtained with *Synechococcus* sp. PCC 7942 cell suspension continuously illuminated with the blue (at 464 nm, panel A) and the orange (622 nm, panel B) actinic light. Fluorescence intensities are plotted in terms of iso-emissive contours that are actually two-dimensional renderings of Fig. 3A and B.

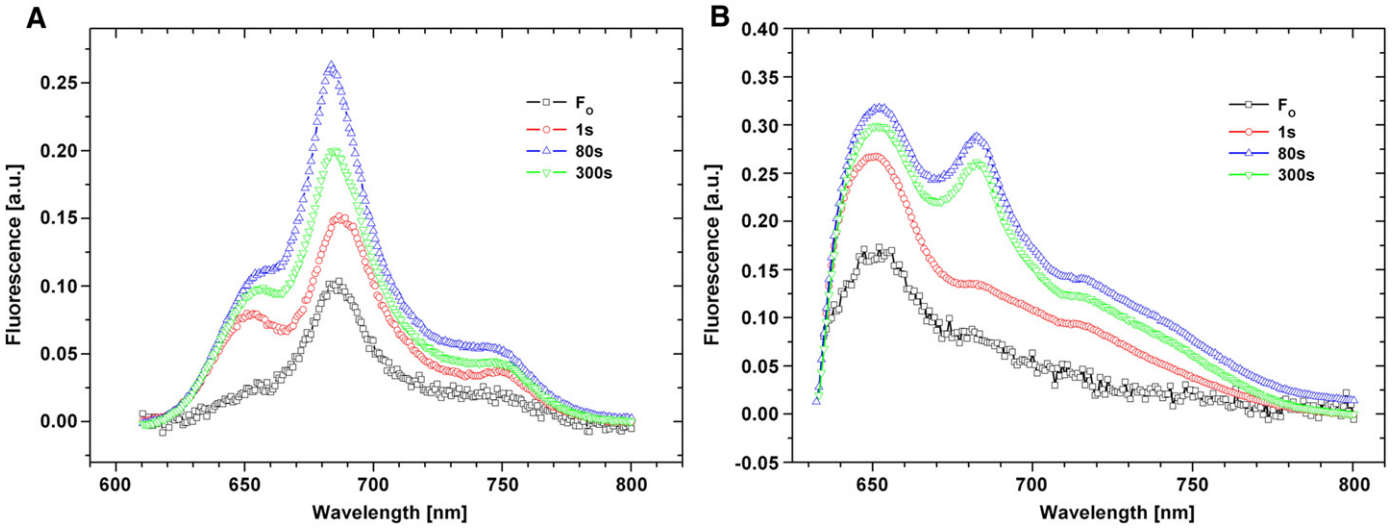

Fig. 5. Fluorescence spectra at characteristic phases (times) of fluorescence induction. The spectra were recorded with continuous blue (464 nm, panel A) and orange (622 nm, panel B) actinic light excitation. They correspond to sections of Fig. 3 landscapes (parallel to the wavelength-fluorescence intensity axes) or of Fig. 4 contour maps (parallel to the wavelength axis). Approximate correspondence of the spectra to the FI phases, as labeled in Fig. 2, are as follows: F_o (dark adapted cells, open circles, black curve) to the O level; 1 s (open circles, red curve) to the S level; 80 s (triangles, blue curve) to the M level; and 300 s (upside down triangles, green curve) to the T level. The intensity of exciting light was the same as in Fig. 3.

bands (F710, F745). Moreover, the pronounced changes in the F650 emission band reflecting CPC emission from phycobilisomes are clearly visible for both the blue and the orange light excitation, since kinetics of F650 band was detectable even under blue excitation (Fig. 5). The position of other bands (F685, F710, F745) is comparable with those obtained by Ivanov et al. [32] on *Synechococcus* PCC 7942 cells measured at 77 K. We have performed similar experimental spectra deconvolution also for our measurements at room temperature; the analysis has resulted in 4 main bands: F650, F685, F710 and F745 for blue (464 nm) and for orange excitation (622 nm) light with parameters presented in Table 1. The results of spectral deconvolution for orange light excitation (Table 1) can be compared with those obtained by Ma et al. [33] for *Synechocystis* sp PCC 6803. In both cases (excitation by blue and orange light), our room temperature spectra did not show the F692–702 bands and the position of F721 reflecting mostly PS I fluorescence was blue shifted to F710.

3.5. The slow fluorescence induction kinetics at particular wavelengths: the SMT transient

In order to obtain an insight into the fate of phycobilin and PS I and PS II emission during FI at room temperature, we made use of the deconvolution of the experimental spectra. The kinetics of individual Gaussian components (amplitudes of F650, F685, F710 and F745) for the blue (464 nm) and orange (622 nm) light excitation are presented in Fig. 6A and B, respectively. The amplitudes are normalized to the amplitudes of particular bands of the F_o spectrum.

Fig. 6 shows that the main Chl a emission band of PS II (F685) follows the typical OPSMT kinetics either with the blue light (464 nm; panel A) or with the orange light (622 nm; panel B). The similar, although not identical, OPSMT kinetics has been found also for the far-red satellite band (F745) of PSII chlorophylls, however with absolute changes much smaller than for the F685 band (data not shown). These two time courses (F685 and F745) were kinetically similar to those shown in Fig. 2 for both types of irradiances. This was not the case for the F710 band reflecting mostly PSI emission and the phycobilisome emission band (F650) that behave differently for blue and orange light excitation. The absolute intensities of the F710 band for the blue and for the orange excitations were much smaller than those of the F685 band (data not shown). However, after normalization to F_o level an increase of the F650 and F710 fluorescence to their maximum was visible. In the case of blue light excitation the initial increase in the PSI fluorescence (F710) and in phycobilisome fluorescence (F650) was followed by slight decrease. The blue light induced SMT phase of F650 and F710 bands was not synchronous with that emitted by Chl a of PS II (F685 and F745) as they occur 20s later. This suggests that the SMT kinetics of the F650 (and F710) bands were not caused just by F685 admixture. The direct interpretation of changes in the F710 fluorescence band, where mostly chlorophylls of PSI but also of PSII contribute cannot be made directly without further experimentation, as the absolute changes in the deconvoluted F710 signal were rather small (data not shown). On the other hand, more pronounced variation in the F650 band provides the first report of light-inducible changes of phycobilin fluorescence *in vivo* during FI, excited by blue light (see Discussion).

4. Discussion

We have explored a spectrally resolved fluorescence induction (i.e. $F_t = \Phi(\lambda,t)$ function) of *Synechoccocus sp.* PCC7942. Mimuro [34]) had earlier summarized the use of such graphs during picosecond time

Table 1
Parameters of fluorescence emission spectra deconvolution.

Excitation	Emission	F650	F685	F710	F745
464 nm	λ	653.8 ± 0.8	685.0 ± 0.7	708.2 ± 2.0	744.0 ± 1.8
	FWHM	13.8 ± 0.3	10.4 ± 0.4	12.4 ± 1.0	17.4 ± 1.3
622 nm	λ	651.2 ± 0.4	682.0 ± 0.8	711.5 ± 0.8	741.0 ± 1.1
	FWHM	11.7 ± 0.6	11.9 ± 0.7	15.2 ± 1.5	21.8 ± 3.3

Four Gaussians were used to fit the experimental curves measured at room temperature *in vivo* (raw data presented in Figs. 3 and 4). This table represents average wavelength (λ) locations, and bandwidths (FWHM — full width at half maximum) of particular bands (F650, F685, F710 and F745), used for deconvolution at various times during fluorescence induction. Data represents $n = 15$ deconvolutions (see Supplementary material for raw fitting data).

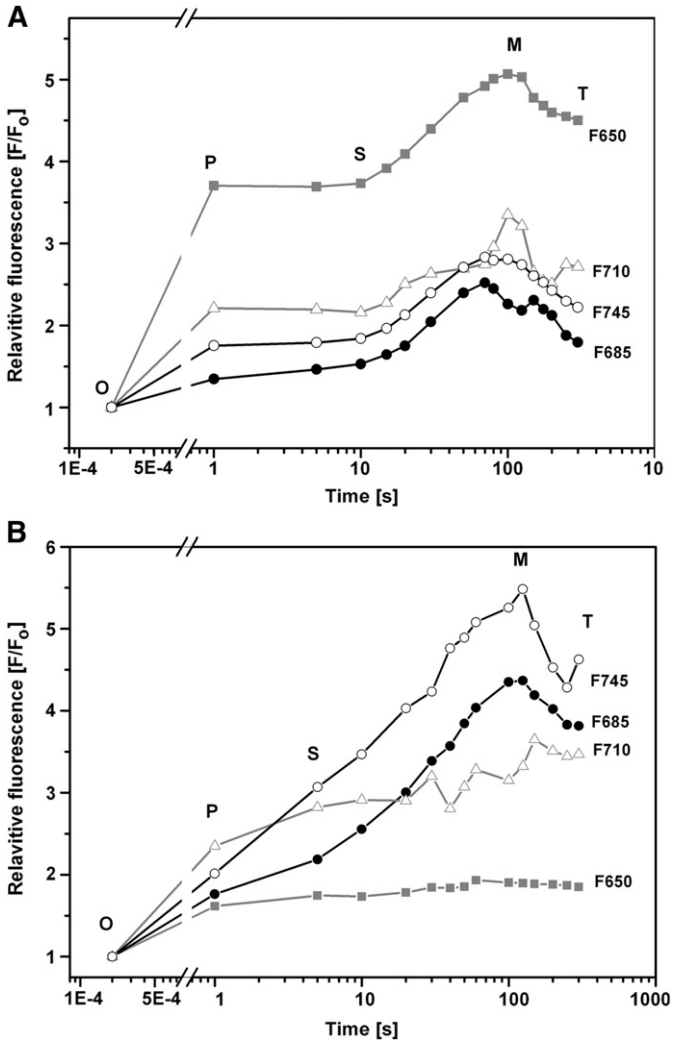

Fig. 6. Fluorescence induction of the main fluorescence band in PCC 7942. Data represent maximum amplitudes of the Gaussian components obtained from deconvolution of the experimental data (see Fig. 3) into the four bands: F650 (allophycocyanin emission of phycobilins); F685 (PSII chlorophylls a); F710 (vibration satellite of PSI chlorophylls) and F745 (vibration satellite of PSII chlorophylls). The blue (464 nm; ~200 μmol(photons) m^{-2} s^{-1} — panel A) and orange (622 nm; ~33 μmol(photons) m^{-2} s^{-1} — panel B) actinic illumination was used. The presented maximum amplitudes of the Gaussian components are normalized to their appropriate values obtained from the F_o spectrum deconvolution, measured with a weak excitation (0.5 μmol(photons) m^{-2} s^{-1}) before the actinic light was turned on. The nomenclature of time points (O P S M and T) is as in Fig. 2. The F/Fo values reported above are too high because the Fo values were not corrected for light intensity, but this does not affect the shapes of the curves shown here.

scales where excitation energy transfer steps were measured. Likewise, Strasser [35; also see 36] had also used 3-dimensional displays for the Chl *a* fluorescence of higher plant leaves (however, of the $F_\lambda = f(\lambda_F, \lambda_E)$ type, where λ_E is the excitation wavelength) in order to analyse the phenomenon of the spillover of electronic excitation from PS II Chl *a* holochromes to those of PS I during the transition from state 1 to 2. Here, we have extended these methods to longer time scale where electron transfer and state changes control fluorescence changes. This three-dimensional curve provides a panoramic view of the time-dependent and wavelength-dependent changes of the fluorescence emission of the main cyanobacterial pigment–protein complexes (PS II, PS I, PBS) during continuous actinic illumination *in vivo*. Typically, FI is measured only in a narrow spectral band (~690–710 nm) where the emission of the Chls *a* that are embedded in PS II predominates. In PBS-containing cyanobacteria, these kinetics obey a characteristic pattern that consists of the initial OJIPS transient (~1–2 s) followed by the slower SMT transient (~several min; see Fig. 2). In this work, we have spectrally resolved the slower SMT phase of FI.

We show in Fig. 2, that the typical OJIPS-SMT fluorescence kinetic pattern is elicited not only by orange actinic illumination, that is directed primarily to the PBS phycobilins, but also by blue actinic illumination that is directed primarily to the Chls *a* of both photosystems, and where CPC [19,20,22] and APC [23] almost do not absorb. The somewhat steeper SM rise and the earlier occurrence of M in the FI pattern recorded with the blue actinic light (Fig. 2) can simply be due to its higher intensity compared to the orange actinic light used in the experiment (see the legend of Fig. 2). However, the SM rise reflects not only the state 2 to state 1 transition (as a consequence of events initiated by the oxidation of the PQ-pool), but is also partly due to the suppression of photochemical quenching (reduction of Q_A and of the PQ-pool) and non-photochemical quenching that depends on the light quality in cyanobacterium (Ref. [1]). Generally, the PQ-pool oxidation proceeds faster with the blue actinic light compared to the orange actinic light because the PS I RCs turn over faster than the PS II RCs [13,37]. This is due to the higher Chl *a* content of PS I compared to PS II in cyanobacteria [29–31]. Fluorescence rise is governed not only by the suppression of the photochemical quenching, but also the non-photochemical quenching. To explain the kinetic differences in the FI curves in Fig. 2, we speculate that the photochemical de-quenching may be more significant for the SM rise in orange light (622 nm) than in blue (464 nm) light.

The spectral analysis of the fluorescence kinetics that we have elaborated in this paper (Figs. 3, 4 and 5) broadens our understanding of the FI phenomenology in the case of the PBS-containing cyanobacteria. Analysis of the serial emission spectra (Fig. 5) into Gaussian components and time plots of the intensities of the Gaussian sub-bands (Fig. 6) reveal the occurrence of SMT-like kinetic patterns not only for the Chl *a* fluorescence (F685) but also for the CPC fluorescence (F650) for the blue (464 nm) actinic excitation. In the classical approach, the SM rise of Chl a FI has been assigned mostly to an increased PBS → PS II excitation transfer. Therefore, the SM rise is a manifestation of the light induced regulation of the PBS excitation redistribution from PS I to PS II (or state 2-to-1 transition). This is possible because the PBS-containing cyanobacteria tend to stay in the weakly fluorescent state 2 during the dark pre-adaptation and transit into the highly fluorescent state 1 during actinic illumination (see Ref. [1], and citations therein). Our experimental approach has brought new possibilities to the analysis of the state transition phenomenonelogy.

Two possible state transition mechanisms have been proposed in cyanobacteria: (1) reversible PBS movement between PS II and PS I (see e.g. [14,38–40] for further details); (2) intramembranous transfer of excitation from Chl *a* holochromes of PS II to Chl *a* holochromes of PS I with no direct involvement of PBS movement — the so-called spill-over mechanism (see e.g. [18,41]) or combination of both [42–44]. In contrast to higher plants and green algae, our knowledge about the state

Table 2
Relative PBS fluorescence intensity at characteristic times of induction.

Excitation	Emission	Time			
		0 s (O)	1 s (P)	80 s (M)	240 s (T)
464 nm	F650/F685	0.22	0.57	0.41	0.47
	F650/F710	0.63	1.22	1.14	1.22
622 nm	F650/F685	2.07	1.93	1.08	1.09
	F650/F710	3.15	2.70	2.22	2.23

The intensities of PBS fluorescence (F650) were taken from the Fig. 3 data. The values represent maximum of PBS fluorescence (F650) normalized to the fluorescence maximum of PS I Chl *a* (F650/F710). The fluorescence intensity ratios for blue light excitation (464 nm, ~200 μmol(photons) m^{-2} s^{-1}) or orange light excitation (622 nm, ~33 μmol(photons) m^{-2} s^{-1}), are presented. O, P, S, M, T represent the different FI phases (at corresponding times in s). The same results have been obtained also for ratios of deconvoluted bands presented in Fig. 6.

transitions mechanism in cyanobacteria is fragmentary. In plants and green algae, state transitions cause reversible phosphorylation–dephosphorylation of light-harvesting LHCII polypeptides; and this is essential for the process [45]. In PBS-containing cyanobacteria and red algae, on the other hand, no light-regulated phosphorylation of the PS II core polypeptides takes place [46]. In cyanobacteria, the phosphorylation of phycobilisomes seems to have quite a different role [47] and also inhibitor of phosphorylation reaction does not have an effect on the SM fluorescence rise [48]. Even though a direct mechanism of state transition triggering is not known, it seems to be controlled by redox state of electron carriers between PS II and PS I [49].

Measurements of fluorescence spectra during the SM rise reflecting state 2 to state 1 transition have shown (Fig. 6): (i) a slight S-M-T increase in the F710 band attributed mostly to PS I emission; (ii) significant SM rise of PS II fluorescence (F685) that is in line with standard FI measurement presented in Fig. 2; (iii) pronounced increase in PBS fluorescence with SMT pattern for blue light excitation (Fig. 6A), and with gradual increase of the F650 band a maximum with orange excitation (Fig. 6B). The F650 changes cannot be simply attributed to F685 admixture as the Fig. 6 represents deconvoluted data. The different origin of F650 and F685 changes is also indicated by their different SMT kinetics for F685 and F650 (Fig. 6). Some older work has already pointed out on the F650 fluorescence increase [48], however our result is the first observation of the stimulation of PBS fluorescence with SMT pattern (i.e. including SM rise and ST decline) under normal conditions *in vivo*.

There are only few papers dealing with the phenomenon of changes in PBS fluorescence *in vivo*. Similar increases in PBS fluorescence has been attributed to PBS decoupling in cyanobacteria at low temperatures [50], at high temperatures (or high light) [51] or under oscillating light [52]. It has been also documented in red algae that contain PBS [53] and in cryptophytes [54,55] that contain special types of phycoerythrins. Snyder and Biggins [54] had proposed that such decoupling may reflect a photoprotective mechanism that may be triggered by changes in the pH of the lumen. In the case of cyanobacteria, the reverse process (coupling of PBS to PS II) seems to be connected with the formation of an active water-oxidizing complex in PS II [56]. Therefore PBS decoupling seems to be a general mechanism for avoiding overexcitation and possible PS II photodamage during conditions of rapidly changing ambient light intensities [51,56].

Another noteworthy observation, in this paper, concerns relative changes in the PBS fluorescence (F650 band) in comparison with the PS II (F685 band) and PS I (F710 band) fluorescence (see Table 2). Quite frequently the cyanobacterial emission spectra are interpreted by normalizing fluorescence intensities at ~650 nm. Here, in the case of blue light excitation, the F650 signal almost doubled in comparison to the F685 and F710 emissions (cf. F650/685 and F650/710 ratios, Table 2). On the other hand, the PBS emission relatively declined to half in comparison to F685 and F710 emission when excited by orange light (Table 2). Our results indicate that we must be cautious of such a normalization process because PBS fluorescence also changes.

The Table 2 also indicates different changes in excitation energy flow during FI for blue and orange light excitations (its relative stimulation by blue light and reduction by orange light). This could indicate a possible role of blue light induced non-photochemical quenching recently proposed in cyanobacteria (reviewed by Kirilovsky [57]) that is controlled by specific cytoplasmic orange carotenoid protein (OCP). The detailed mechanism behind such a process is still under extensive research [58,59]. However it has been shown that *Synechococcus* sp. PCC 7942 does not have a gene coding OCP protein [60]. This indicates that blue light induced quenching regulated by OCP protein is not involved in the observed relative increase in F650 fluorescence (see F650/F685 ratios in Table 2).

The photoinduced, reversibly variable F650 fluorescence, discussed in this paper, would certainly require considering additional mechanisms. It is a challenging and tempting phenomenon for further investigations. Instead of speculating on the possible mechanisms, we prefer to keep it as our goal for future research. We expect the answers to come from further research on the application of our approach to other organisms with different regulation and organization of light harvesting.

Note Added in Proofs

While correcting our proofs, we became aware of a very recent paper (by Küpper and coworkers [61]), relevant to our studies, showing reversible phycobilisome (PBS) uncoupling (resulting in changes in PBS fluorescence) during cell cycle of a nitrogen fixing cyanobacterium Trichodesmium. We expect, in the future, to compare these data with similar data obtained with cyanobacteria containing Pcb-type light-harvesting antennae, as well as with algae and higher plants.

Acknowledgements

Govindjee thanks Ladislav Nedbal, Ondřej Prášil and Ivan Šetlik for their hospitality when this work was initiated in Nové Hrady and Třeboň; he is also thankful to the support received from Feng Sheng Hu, Head of Plant Biology, at the University of Illinois at Urbana-Champaign, during the preparation of this manuscript. The project has been supported by GAČR 206/09/094 and by GAČR 206/07/0917. O.P. and R.K. were supported by research grants (GAAV A608170603 and the Institutional Research Concepts AV0Z50200510 and MSM6007665808).

Appendix A. Supplementary data

Supplementary data associated with this article can be found, in the online version, at doi:10.1016/j.bbabio.2009.04.013.

References

[1] G.C. Papageorgiou, M. Tsimilli-Michael, K. Stamatakis, The fast and slow kinetics of chlorophyll a fluorescence induction in plants, algae and cyanobacteria: a viewpoint, Photosynth. Res. 94 (2007) 275–290.
[2] W.S. Chow, A. Melis, J.M. Anderson, Adjustment of photosystem stoichiometry in chloroplasts improves the quantum efficiency of photosynthesis, Proc. Natl. Acad. Sci. U. S. A. 87 (1990) 7502–7506.
[3] E. Tyystjärvi, I. Vass, Light emission as a probe of charge separation and recombination in the photosynthetic apparatus: relation of prompt fluorescence to delayed light emission and thermoluminescence, in: G.C. Papageorgiou, Govindjee (Eds.), Advances in Photosynthesis and Respiration, Vol. 19, Chlorophyll Fluorescence: a Signature of Photosynthesis, Springer, Dordrecht, 2004, pp. 363–388.
[4] D. Bruce, S. Vasil'ev, Excess light stress: multiple dissipative processes of excess excitation, in: G.C. Papageorgiou, Govindjee (Eds.), Advances in Photosynthesis and Respiration, Vol. 19, Chlorophyll Fluorescence: a Signature of Photosynthesis, Springer, Dordrecht, 2004, pp. 497–523.
[5] D.M. Kramer, T.J. Avenson, A. Kanazawa, J.A. Cruz, B. Ivanov, G. Edwards, The relationship between photosynthetic electron transfer and its regulation, in: G.C. Papageorgiou, Govindjee (Eds.), Advances in Photosynthesis and Respiration, Vol. 19, Chlorophyll Fluorescence: a Signature of Photosynthesis, Springer, Dordrecht, 2004, pp. 252–278.
[6] C.W. Mullineaux, D. Emlyn-Jones, State transitions: an example of acclimation to low-light stress, J. Exp. Bot. 56 (2005) 389–393.
[7] Govindjee, Sixty-three years since Kautsky: chlorophyll a fluorescence, Aust. J. Plant Physiol. 22 (1995) 131–160.
[8] D. Lazár, The polyphasic chlorophyll a fluorescence rise measured under high intensity of exciting light, Funct. Plant Biol. 33 (2006) 9–30.
[9] R.J. Strasser, M. Tsimilli-Michael, A. Srivastava, Analysis of the chlorophyll a fluorescence transient, in: G.C. Papageorgiou, Govindjee (Eds.), Advances in Photosynthesis and Respiration, Vol. 19, Chlorophyll Fluorescence: a Signature of Photosynthesis, Springer, Dordrecht, 2004, pp. 321–362.
[10] R. MacColl, Cyanobacterial phycobilisomes, J. Struct. Biol. 124 (1998) 311–334.
[11] N. Adir, Elucidation of the molecular structures of components of the phycobilisome: reconstructing a giant, Photosynth. Res. 85 (2005) 15–32.
[12] A.N. Glazer, Phycobilisome: a macromolecular complex optimized for energy transfer, Biochim. Biophys. Acta 768 (1984) 29–51.
[13] K. Stamatakis, M. Tsimilli-Michael, G.C. Papageorgiou, Fluorescence induction in the phycobilisome-containing cyanobacterium *Synechococcus* sp PCC 7942: analysis of the slow fluorescence transient, Biochim. Biophys. Acta 1767 (2007) 766–772.

[14] M. Tsimilli-Michael, K. Stamatakis, G.C. Papageorgiou, Dark-to-light transition in *Synechococcus* sp. PCC 7942 cells studied by fluorescence kinetics assesses plastoquinone redox poise in the dark and photosystem II fluorescence component and dynamics during state 2 to state 1 transition, Photosynth. Res. 99 (2009) 243–255.
[15] R. Ripka, J.B. Waterbury, R.Y. Stanier, Isolation and purification of cyanobacteria; some general principles, in: M.P. Starr, H. Stolp, H.G. Truper, A. Balows, H.G. Schlegel (Eds.), The Prokaryotes, Springer-Verlag, Berlin, 1981, pp. 212–220.
[16] M.D. Trtílek, M. Kramer, M. Koblížek, L. Nedbal, Dual modulation LED kinetic fluorometer, J. Luminescence 72–74 (1997) 597–599.
[17] H. Scheer, The pigments, in: B.R. Green, W.W. Parson (Eds.), Advances in Photosynthesis and Respiration, Vol. 13, Light Harvesting Antennas, Kluwer Academic Publishers, Dordrecht, 2003, pp. 29–81.
[18] PapageorgiouG.C. , Fluorescence of photosynthetic pigments in vitro and in vivo, in: G.C. Papageorgiou, Govindjee (Eds.), Advances in Photosynthesis and Respiration, Vol. 19, Chlorophyll Fluorescence: a Signature of Photosynthesis, Springer, Dordrecht, 2004, pp. 43–63.
[19] V.T. Oi, A.N. Glazer, L. Stryer, Fluorescent phycobiliprotein conjugates for analyses of cells and molecules, J. Cell Biol. 93 (1982) 981–986.
[20] G. Patil, S. Chethana, A.S. Sridevi, K.S.M.S. Raghavarao, Method to obtain C-phycocyanin of high purity, J. Chromatogr. 1127 (2006) 76–81.
[21] S.P. Zhang, J. Xie, J.P. Zhang, J.Q. Zhao, L.J. Jiang, Electron spin resonance studies on photosensitized formation of hydroxyl radical by C-phycocyanin from *Spirulina platensis*, Biochim. Biophys. Acta 1426 (1999) 205–211.
[22] J. Gysi, H. Zuber, Isolation and characterization of allophycocyanin II from the thermophilic blue-green alga *Mastigocladus laminosus* Cohn. FEBS Lett. 48 (1974) 209–213.
[23] R. MacColl, K. Csatorday, D.S. Berns, E. Traeger, Chromophore interactions in allophycocyanin, Biochemistry 19 (1980) 2817–2820.
[24] E.G. Andrizhiyevskaya, A. Chojnicka, J.A. Bautista, B.A. Diner, R. van Grondelle, J.P. Dekker, Origin of the F685 and F695 fluorescence in photosystem II, Photosynth. Res. 84 (2005) 173–180.
[25] E.G. Andrizhiyevskayaa, T.M.E. Schwabe, M. Germano, S. D Haene, J. Kruip, R. van Grondelle, J.P. Dekker, Spectroscopic properties of PSI–IsiA supercomplexes from the cyanobacterium *Synechococcus* PCC 7942, Biochim. Biophys. Acta 1556 (2002) 265–272.
[26] A.N. Glazer, D.A. Bryant, A new cyanobacterial phycobiliprotein, Arch. Microbiol. 104 (1975) 15–22.
[27] F. Franck, P. Juneau, R. Popovic, Resolution of the photosystem I and photosystem II contributions to chlorophyll fluorescence of intact leaves at room temperature, Biochim. Biophys. Acta 1556 (2002) 239–246.
[28] S. Itoh, K. Sugiura, Fluorescence of photosystem I, in: G.C. Papageorgiou, Govindjee (Eds.), Advances in Photosynthesis and Respiration, Vol. 19, Chlorophyll Fluorescence: a Signature of Photosynthesis, Springer, Dordrecht, 2004, pp. 231–250.
[29] P. Jordan, P. Fromme, H.T. Witt, O. Klukas, W. Saenger, N. Krauss, Three-dimensional structure of cyanobacterial photosystem I at 2.5 Å resolution, Nature 411 (2001) 909–917.
[30] B. Loll, J. Kern, W. Saenger, A. Zouni, J. Biesiadka, Towards complete cofactor arrangement in the 3.0 Å resolution structure of photosystem II, Nature 438 (2005) 1040–1044.
[31] Y. Fujita, A. Murakami, K. Aizawa, K. Ohki, Short-term and long-term adaptation of the photosynthetic apparatus: homeostatic properties of thylakoids, in: D.A. Bryant (Ed.), Advances in Photosynthesis and Respiration, Vol. 1, The Molecular Biology of Cyanobacteria, Kluwer Academic Publishers, Dordrecht, 1994, pp. 677–692.
[32] A.G. Ivanov, A. Krol, E. Selstam, P.V. Sane, D. Sveshnikov, Y.-I. Park, G. Öquist, N.P.A. Huner, The induction of CP43′ by iron-stress in *Synechococcus* sp. PCC 7942 is associated with carotenoid accumulation and enhanced fatty acid unsaturation, Biochim. Biophys. Acta 1767 (2007) 807–813.
[33] W. Ma, L. Chen, L. Wei, Q. Wang, Excitation energy transfer between photosystems in the cyanobacterium *Synechocystis* 6803, J. Luminiscence 126 (2008) 546–548.
[34] M. Mimuro, Visualization of excitation energy transfer processes in plants and algae, Photosynth. Res. 73 (2002) 133–138.
[35] StrasserR.J. , Mono, -bi, tri, and poly-partite models in photosynthesis, Photosynth. Res. 10 (1986) 255–276.
[36] LombardF. , StrasserR.J. , Evidence of spill over changes during state-1 to state-2 transition, in: C. Sybesma (Ed.), Advances in Photosynthesis Research, Proceedings of the VI th Congress on Photosynthesis, Brussels, Belgium 1983, III, Martinus Nijhoff/Dr. W. Junk Publishers, The Hague, 1984, pp. 271–274.
[37] S. Savikhin, Ultrafast optical spectroscopy of photosystem I, in: J.H. Golbeck (Ed.), Photosystem I: the Light-Driven Plastocyanin: Ferredoxin Oxidoreductase. Advances in Photosynthesis and Respiration, Vol. 24, Springer, Dordrecht, 2006, pp. 155–175.
[38] C.W. Mullineaux, M.J. Tobin, G.R. Jones, Mobility of photosynthetic complexes in thylakoid membranes, Nature 390 (1997) 421–424.
[39] S. Joshua, C.W. Mullineaux, Phycobilisome diffusion is required for light-state transitions in cyanobacterial, Plant Physiol. 135 (2004) 2112–2119.
[40] D.H. Li, J. Xie, J.Q. Zhao, A.D. Xia, D.H. Li, Y.D. Gong, Light-induced excitation energy redistribution in *Spirulina platensis* cells: "spillover" or "mobile PBSs"? Biochim. Biophys. Acta 1608 (2004) 114–121.
[41] D. Bruce, S. Brimble, D.A. Bryant, State transitions in a phycobilisomes less mutant of the cyanobacterium *Synechococcus* sp. PCC 7002, Biochim. Biophys. Acta. 974 (1989) 66–73.
[42] M. Koblížek, J. Komenda, J. Masojidek, State transitions in the cyanobacterium *Synechococcus* PCC7942. Mobile antenna or spillover? in: G. Garab (Ed.), Photosynthesis: Mechanisms and Effects, Kluwer Academic Publishers, Dordrecht, 1998, pp. 213–216.
[43] M.D. McConnell, R. Koop, S. Vasil ev, D. Bruce, Regulation of the distribution of chlorophyll and phycobilin-absorbed excitation energy in cyanobacteria. A structure based model for the light state transition, Plant Physiol. 130 (2002) 1201–1212.
[44] H. Li, D.H. Li, S.Z. Yang, H. Xie, J.Q. Zhao, The state transition mechanism — simply depending on light-on and -off in *Spirulina platensis*, Biochim. Biophys. Acta 1757 (2006) 1512–1519.
[45] M. Tikkanen, M. Nurmi, M. Suorsa, R. Danielsson, F. Mamedov, S. Styring, E.M. Aro, Phosphorylation-dependent regulation of excitation energy distribution between the two photosystems in higher plants, Biochim. Biophys. Acta 1777 (2008) 425–432.
[46] S. Pursiheimo, E. Rintamaki, E. Baena-Gonzalez, E.M. Aro, Thylakoid protein phosphorylation in evolutionally divergent species with oxygenic photosynthesis, FEBS Lett. 423 (1998) 178–182.
[47] I. Piven, G. Ajlani, A. Sokolenko, Phycobilisome linker proteins are phosphorylated in *Synechocystis* sp PCC 6803, J. Biol. Chem 280 (2005) 21667–21672.
[48] G. Papageorgiou, Govindjee, Light induced changes in the fluorescence yield of chlorophyll a in vivo. I. *Anacystis nidulans*, Biophysic. J. 8 (1968) 1299–1315.
[49] C.W. Mullineaux, J.F. Allen, State-1–state-2 transitions in the cyanobacterium *Synechococcus* 6301 are controlled by the redox state of electron carriers between photosystem-I and photosystem-II, Photosynth. Res. 23 (1990) 297–311.
[50] U. Schreiber, Reversible uncoupling of energy-transfer between phycobilins and chlorophyll in *Anacystis nidulans* — light stimulation of cold-induced phycobilisome detachment, Biochim. Biophys. Acta 591 (1980) 361–371.
[51] K. Stoitchkova, O. Zsiros, T. Javorfi, T. Pali, A. Andreeva, Z. Gombos, G. Garab, Heat- and light-induced reorganizations in the phycobilisome antenna of *Synechocystis* sp PCC 6803. Thermo-optic effect, Biochim. Biophys. Acta 1767 (2007) 750–756.
[52] L. Nedbal, V. Brezina, F. Adamec, D. Stys, V. Oja, A. Laisk, G. Govindjee, Negative feedback regulation is responsible for the non-linear modulation of photosynthetic activity in plants and cyanobacteria exposed to a dynamic light environment, Biochim. Biophys. Acta 1607 (2003) 5–17.
[53] L.-N. Liu, A.T. Elmalk, T.J. Aartsma, J.-C. Thomas, B. Lamers, C.H. Zhou, Y.-Z. Zhang, Light-induced energetic decoupling as a mechanism for phycobilisome-related energy dissipation in red algae: a single molecule study, PLoS ONE 3 (9) (2008) e3134.
[54] U.K. Snyder, J. Biggins, Excitation-energy redistribution in the cryptomonad alga *Crytomonas ovata*, Biochim. Biophys. Acta 892 (1987) 48–55.
[55] R. Kaňa, O. Prášil, C. Mullineaux, Immobility of phycobilins in the thylakoid lumen of a cryptophyte suggests that protein diffusion in the lumen is very restricted, FEBS Lett. 583 (2009) 670–674.
[56] H.J. Hwang, A. Nagarajan, A. McLain, R.L. Burnap, Assembly and disassembly of the photosystem II manganese cluster reversibly alters the coupling of the reaction center with the light-harvesting phycobilisome, Biochemistry 47 (2008) 9747–9755.
[57] D. Kirilovsky, Photoprotection in cyanobacteria: the orange carotenoid protein (OCP)-related non-photochemical-quenching mechanism, Photosynth. Res. 93 (2007) 7–16.
[58] M. Rakhimberdieva, I. Stadnichuk, I. Elanskaya, N. Karapetyan, Carotenoid-induced quenching of the phycobilisome fluorescence in photosystem II-deficient mutant of *Synechocystis* sp. PCC 6803, FEBS Lett. 574 (2004) 85–88.
[59] M. Scott, C. McCollum, S. Vasil'ev, C. Crozier, G.S. Espie, M. Krol, N.P.A. Huner, D. Bruce, Mechanism of the down regulation of photosynthesis by blue light in the cyanobacterium *Synechocystis* sp. PCC 6803, Biochemistry 45 (2006) 52–89.
[60] C. Boulay, L. Abasova, Ch. Six, I. Vass, D. Kirilovsky, Occurrence and function of the orange carotenoid protein in photoprotective mechanisms in various cyanobacteria, Biochim. Biophys. Acta 1777 (2008) 1344–1354.
[61] H. Küpper, E. Andresen, S. Wiegert, S. Miloslav, B. Leitenmaier, I. Šetlík, Reversible coupling of individual phycobiliprotein isoforms during state transitions in the cyanobacterium Trichodesmium analysed by single-cell fluorescence kinetic measurements, Biochim. Biophys. Acta 1787 (2009) 155–167.

Abbreviations

APC: allophycocyanin
CPC: C-phycocyanin
Chl: chlorophyll
FWHM: Full width at half maximum
FI: fluorescence induction
F_m (F_o)*:* maximal (minimal) variable chlorophyll a fluorescence
F685: fluorescence band with a peak at ~ 685–686 nm
F650: fluorescence band with a peak between ~ 650 and 654 nm
F710: fluorescence band with a peak between ~ 710 and 720 nm
F745: fluorescence band with a peak between ~ 710 and 720 nm
$F_{690-710}$*:* fluorescence measured by commercial instruments in the wavelength region of 690–710 nm
OCP: orange carotenoid protein
PAR: photosynthetic active radiation
PS I (II): Photosystem I (II)
PS II RC: PS I RC, reaction centers of PS II, PSI
PBS: phycobilisome